IONETIX

N-13 AMMONIA

Accessible. Affordable. Available now.

IONETIX.com

The Rationale for Employing ^{13}N-Ammonia PET/CT Regadenoson Stress MPI in the Evaluation of Chest Pain through the Emergency Department

The University of Kansas Hospital System Experience

University of Kansas Medical Center

Thomas Rosamond, MD, Wendell Yap, MD, and Joe Donald, MD

Identifying a "best in class" tracer for evaluating chest pain in the Emergency Department (ED)

When a patient presents in the ED with chest pain or shortness of breath, physicians need timely access to the accurate data provided by noninvasive imaging of myocardial perfusion and function. The authors of this white paper explore the case for utilizing N-13 Ammonia for cardiac stress testing through the ED and describe their experience starting a laboratory for that purpose.

A WHITE PAPER

The rationale for employing ^{13}N-Ammonia PET/CT Regadenoson stress MPI in the evaluation of chest pain through the emergency department

The University of Kansas Hospital System Experience

Thomas Rosamond, MD, Wendell Yap, MD, and Joe Donald, MD.

This white paper elaborates the fundamental first-principles case for utilizing ^{13}N-Ammonia for cardiac stress testing through the emergency department and then describes a real-world experience in starting a laboratory for that purpose from scratch.

^{13}N-Ammonia was approved by the Food and Drug Administration (FDA) on 8/23/2007 as "*a radioactive diagnostic agent for Positron Emission Tomography (PET), for diagnostic PET imaging of the myocardium under rest or pharmacologic stress conditions to evaluate myocardial perfusion in patients with suspected or existing coronary artery disease." (Acceptance letter: NDA 22-119, application No.: 022119).*

Introduction

The evaluation of chest pain in the emergency department (ED) is a frequent, pressing and defining dilemma for the clinician. The stakes, both for the physician and the patient, are as high as any in medicine.[1,2,3,4] Out of necessity, ED physicians turn to the available imaging modalities to assist them in this analysis. In many cases, noninvasive imaging serves as the critical factor physicians rely on to determine whether to discharge the patient from the ED or to admit the patient for evaluation and management in the hospital. It is imperative, therefore, that the tools employed by the physician in this setting are as robust and reliable as can be achieved safely and in a cost- and time-efficient manner.

Regadenoson stress PET/CT myocardial perfusion imaging (MPI) with ^{13}N-Ammonia provides the optimal combination of radiotracer characteristics, efficiency of testing protocol workflow, and supply chain performance for this purpose. Its relatively long half-life and high myocardial extraction fraction, low liver and gut uptake, which can be problematic and common with ^{82}Rb and ^{99m}Tc, as well as rapid blood-pool clearance, make ^{13}N-Ammonia the best available PET myocardial perfusion tracer for imaging and myocardial blood flow (MBF) quantification.[11]

Best in Class Rationale

The case for utilizing ^{13}N-Ammonia PET/CT Regadenoson pharmacological stress MPI through the ED compared to other imaging alternatives runs along five lines of reasoning.

1. ^{13}N-Ammonia Best in Class: Radiation Dosimetry.

The effective radiation dose for ^{13}N-Ammonia studies with standard PET technology and rest-stress protocols are typically 2mSv or less. Typical stress dose for 3D/2D ^{13}N-Ammonia is 10/15 mCi or an effective dose of 2mSv/GBq while with ^{82} RbCl the dose is 30/45mCi with an effective dose of 1mSv/GBq (Table1)[82]. The best estimate for mean effective dose with ^{82}RbCl using the weighting factors of the ICRP103 is 3.7mSv.[84] In the future, further reductions of the administered dose are anticipated for ^{13}N-Ammonia.[83]

TABLE 1
Properties of Radiotracers Used for PET MBF Quantification

Property	^{82}Rb-chloride	^{13}N-ammonia	^{15}O-water	^{18}F-flurpiridaz
Isotope production method	Generator	Cyclotron	Cyclotron	Cyclotron
Isotope half-life (min)	1.27	10	2.0	110
Positron range (mm) RMS	2.6	0.57	1.0	0.23
Image resolution (mm) FWHM	8	5	6	5
Effective dose (mSv/GBq)	1	2	1	20
Peak stress/rest* extraction (%)	35/70	95/100	100	95/100
Peak stress/rest* retention (%)	25/70	50/90	0	55/90
Spillover from adjacent organs	Stomach wall	Liver and lung	Liver	Early liver
Regulatory status	FDA-approved; 2 suppliers	FDA-approved; ANDA required for onsite production	Not FDA-approved	Phase 3 trials partially completed
Typical rest dose for 3D/2D (mCi†)	30/45	10/15	20/30	2/3
Typical stress dose for 3D/2D (mCi†)	30/45	10/15	20/30	6/7
Protocol features	Rapid protocol	Permits exercise‡; delay of 4–5 half-lives between rest and stress unless different doses used	Rapid protocol; no tracer retention for routine MPI	Permits exercise‡; different doses for rest and stress required

*Peak stress = 3–4 mL/min/g, rest = 0.75–1.0 mL/min/g.
†1 mCi = 37 MBq.
‡Exercise protocols do not allow quantification of MBF.
RMS = root mean square (standard) deviation; FWHM = full width at half maximum achievable using PET scanner with 5-mm spatial resolution; FDA = Food and Drug Administration; ANDA = abbreviated new drug application.

2. ^{13}N-Ammonia Best in Class: Myocardial Extraction and Linearity Proportional to Myocardial Blood Flow.

The fundamental *raison d'etre* of myocardial perfusion imaging is the assessment of the heterogeneity of regional myocardial perfusion and its quantification. The ideal perfusion

agent would have high sensitivity to all changes in coronary blood flow and a quantifiable relationship between image signal intensity and myocardial perfusion. All current perfusion tracers other than ^{15}O-water, which is not FDA approved, demonstrate a significant "roll-off" phenomenon at the high flow rates typically achieved with adenosine or Regadenoson stress (arteriolar vasodilatation by endothelial-mediated mechanisms are associated with a 3.5-4.0-fold increase in myocardial blood flow). This results in reduced sensitivity for less severe coronary stenosis and potentially compromised test sensitivity, leading to false negative or Type II errors in the assessment of chest pain in the ED.

The ideal perfusion agent would have first pass extraction fraction close to 1.0 and maintain a linear relationship between myocardial concentration of tracer and relative regional perfusion. First-pass extraction for ^{13}N-Ammonia is nearly 100% compared to only 50-60% for ^{82}Rubidium-Chloride (^{82}RbCl). By comparison, first pass ^{201}Thallous Chloride extraction is 84%, ^{99m}Tc-sestamibi and ^{99m}Tc-tetrofosmin only 64% and 54% respectively.[9] ^{13}N-Ammonia is the **best in class** perfusion agent for this purpose. ^{13}N-Ammonia has the most extended linear range of tracer uptake relative to myocardial blood flow (Fig.2) of all the single-photon emission computerized tomography (SPECT) and PET MPI radiotracers available. ^{13}N-Ammonia also has high myocardial retention and rapid washout from the blood pool, making it the optimal choice to image myocardial flow heterogeneity.

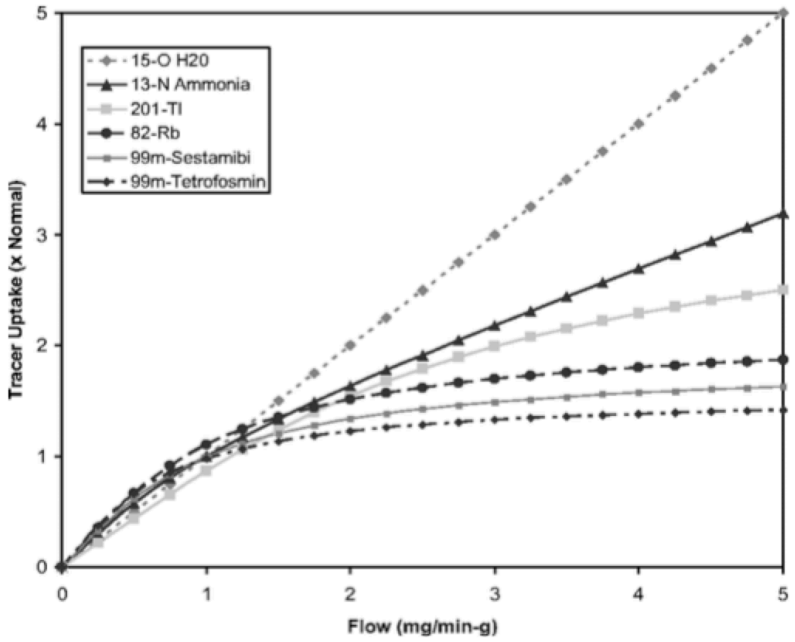

Figure 2. The relationship between myocardial blood flow and percent activity demonstrating a roll-off phenomenon at high flow rates for both SPECT and PET perfusion agents. This results in reduced sensitivity for less severe coronary stenosis. Taken from Salerno M and Bellar G. Noninvasive Assessment of Myocardial Perfusion. Circ Cardiovasc Imaging. 2009; 2:412-424.

3. ^{13}N-Ammonia Best in Class: Spatial Resolution.

The ideal technique would employ tracers that have inherently high spatial resolution so that transmural differences in perfusion could be optimally detected, and the mass and regional distribution of myocardium affected can be more accurately estimated. High count statistics and superior spatial resolution with ^{13}N-Ammonia combine to improve the estimation of arterial input function estimation required for quantitative MBF measurements, which add diagnostic value to evaluating the perfusion images.

With ^{13}N-Ammonia's relatively short positron mean free path, it fundamentally offers the highest spatial resolution of the currently available PET and SPECT tracers (Fig. 3). Spatial resolution values measured (FWHM) are 5 mm for ^{13}N-Ammonia, 8 mm for ^{82}RbCl and approximately 15 mm or greater for the ^{99m}Tc SPECT agents and ^{201}Thallium Chloride.[82] There is no conceivable detector spatial resolution improvement that can overcome this fundamental physical characteristic of the radiotracer employed.

Characteristics of PET Perfusion Tracers: Mean and Maximum Free Path of Positrons Prior To Annihilation
(Maximum and Mean Positron range in millimeters)

Ranges in H2O from Anne Paans Jan 22, 1997 email burst to "nucmed" listserver

Nuclide	Max. Energy (MeV)	Max. Range (mm)	Mean Range (mm)
^{11}C	0.961	3.9	1.1
^{13}N	1.190	5.1	1.5
^{15}O	1.723	8.0	2.5
^{18}F	0.635	2.4	0.6
^{68}Ga	1.899	8.9	2.9
^{82}Rb	3.350	17.0	5.9

The kinetic energy of the positron degrades the special resolution. According to Paans:

> The effect of the kinetic energy on the spacial resolution has been measured for ^{11}C by Phelps et al. by comparison with the 514 keV gamma ray from ^{85}Sr. The effect was a contribution of 1 mm to the spacial resolution, see JNM 16 (1975) 649.
>
> The effect of the kinetic energy on spacial resolution has also been demonstrated by Alan Jeavons and Dave Tomnsend (Geneva) using their HIDAC multi-wire positron system with ^{68}Ga in PTFE tubing or Fe tubing.

AMJ Paans, PET-Center, Groningen University Hospital, Netherlands.

Figure 3. The effect of the kinetic energy and positron range has been demonstrated and can be applied to the currently available radiotracers for PET.

Note by this analysis, ^{82} RbCl's maximum positron range before annihilation is 17 mm. The average thickness of normal left ventricular myocardium in only about 10 mm or less. Compare this to ^{13}N-Ammonia, whose positron range maximum is only 5.1 mm.

Figure 4, below, demonstrates graphically the effect of positron range on endpoint annihilation scatter plots according to each radionuclide emission properties. Only ^{18}F-flurpiridaz, which is not currently available and is not approved by the FDA or available for clinical use, has a tighter scatter plot than ^{13}N-Ammonia, while ^{82}RbCl has the broadest positron scatter plot.

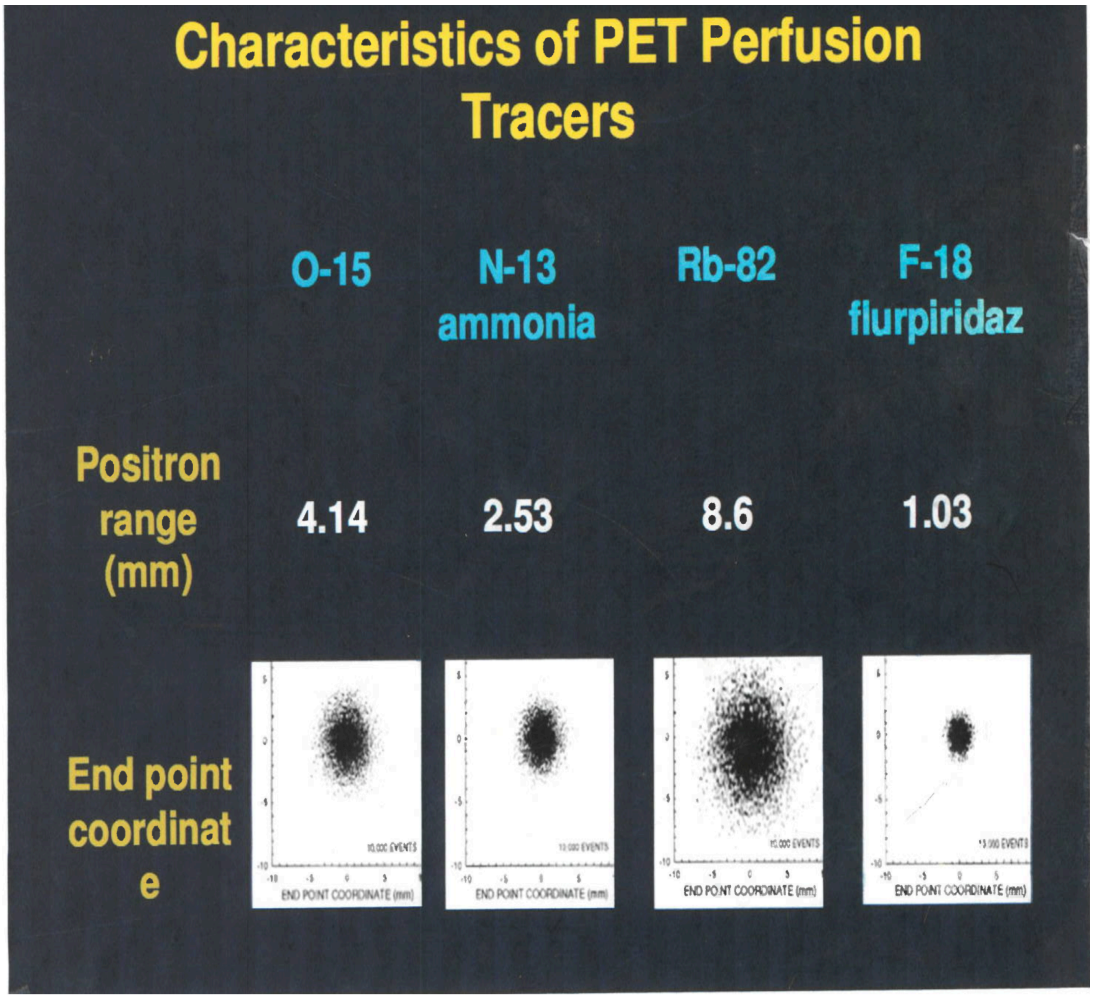

Figure 4. Demonstrates the positron range scatter plots for each radionuclide. ^{13}N-Ammonia has the shortest positron range of the available PET perfusion agents. Maddahi J, circa 2010 ASNC.

4. ^{13}N-Ammonia Best in Class: Quantification of Myocardial Blood Flow.

The clinical objective of combined quantitative and qualitative assessment of myocardial blood flow with PET is to provide physiological, mechanistic, and prognostic information to guide, triage, and tailor therapeutic and invasive therapy to the individual needs of the patient.[75]

The non-invasive quantification of absolute hyperemic myocardial blood flow and flow reserve with PET imaging has been called the "elite" tool for coronary artery detection and offers a "paradigm shift in the management of CAD."[75] ^{13}N-Ammonia is the **best-in-class** radiotracer for this purpose and ***"provides superior image quality and more accurately tracks peak hyperemic myocardial blood flow than ^{82}RbCl."***[74] Detector saturation during the blood-pool phase with ^{82}RbCl can be particularly challenging[82] and coronary flow reserve estimates with ^{82} RbCl may be underestimated compared with ^{13}N-Ammonia.[81] Lowering the administered dose of ^{82}RbCl may lead to poorer statistical quality of the images, which is not typically problematic for ^{13}N-Ammonia.

Most SPECT and PET myocardial perfusion studies are currently reviewed in a visual "artisan approach."[75] Nevertheless, the added value of quantitative myocardial blood flow over qualitative myocardial perfusion has been demonstrated in several studies."[68,69,70,71] The quantitative analysis of relative hypo-perfusion has been shown to rival the accuracy of expert readers in the diagnosis of coronary artery disease utilizing SPECT in large studies.[71] The key advantage of quantitative analysis is the improved reproducibility as compared to even intra-observer variability.[72] Due to variable characteristics of normal perfusion distribution for different tracers, such as the reduced isotope concentration in the lateral wall for the ^{13}N-Ammonia imaging, relative analysis of PET perfusion will require isotope-specific normal limits.[77] PET is currently the most validated imaging technique for the quantitative evaluation of the myocardial blood flow. The quantitative agreement between the different software methods available is very good for ammonia models.[76]

5. ^{13}N-Ammonia Best in Class: Supply Chain Performance.

Any clinician experienced in myocardial perfusion imaging is already well aware of the liabilities of depending upon Technetium labeled flow tracers or ^{82}Strontium/^{82}Rubidium generators for their SPECT or PET clinical applications. In recent memory, there have been several occasions where ^{82,85}Sr breakthrough has sidelined the manufacturers and suppliers of ^{82}Rb generators and exposed their customers to legal liability. The same holds true, even more so, for the Technetium supply chain, which is already precariously stretched around the world from the few remaining nuclear reactors. Reactor shutdowns and supply shortages are like to intensify and become more frequent in the future. A wholesale shutdown of the ^{99}Molybdenum/^{99m}Technetium supply chain would likely result in a run on the available Thallium suppliers, resulting in shortages and delays of its distribution and availability.

Contrast this to the onsite and on-demand production of ^{13}N-Ammonia. Under this scenario, the vulnerable supply chain is eliminated. The local operator/supplier is in control and not dependent upon third party distributors or unreliable manufactures. Once the hurdle of onsite production of ^{13}N-Ammonia based upon demand is overcome, there is little or no reason to prefer the other tracers. We have already demonstrated above the superiority of ^{13}N-Ammonia to all the other FDA-approved radiotracers not only

physiologically, and functionally, but also according to dosimetry, including that of ^{18}F-flurpiridaz.

Summary: Best in Class Rationale

^{13}N-Ammonia, according to its principle physical, radiochemical, physiological and supply-chain performance, offers clear and sustainable advantages over ^{82}RbCl PET/CT MPI, the SPECT ^{99m}Tc-labeled agents or ^{201}Thallous Chloride.

The ^{13}N-Ammonia methodological platform provides physicians with the optimal noninvasive alternative to decrease unnecessary hospital admissions and invasive catheterizations by reducing the frequent false-positive and false-negative liabilities of other non-invasive tests while at the same time delivering the lowest achievable radiation dose to the patient.

Compared to the other nuclear and non-nuclear cardiac testing modalities currently available, MPI combined with quantitative myocardial blood flow analysis with ^{13}N-Ammonia PET/CT delivers the best-in-class combination of technical flexibility, testing accuracy, radiation dose reduction, and supply chain reliability.

Real World Experience: ^{13}N-Ammonia PET/CT MPI

Process design and programmatic implementation: A case study.

Recognizing the limitations and liabilities of standard SPECT imaging and ^{82} Rb PET/CT MPI and in an effort to maximize operational efficiency while simultaneously optimizing length of stay, radiation dose reduction, clinical decision-making, imaging accuracy, reliability, and reproducibility, we embarked on a mission to bring ^{13}N-Ammonia to The University of Kansas Medical Center for the evaluation of chest pain through the ED in February 2020. By mid-May 2020, despite the raging COVID-19 pandemic, we had completed 100 studies for this indication.

To build the service from scratch, we first organized and established our supply chain by contracting with Ionetix Corporation to run the cyclotron residing in the basement of the hospital, which is immediately adjacent to the ED. There is only a 5-minute walk to the hotlab and the PET/CT Discovery MI scanner across the hall.

Our purpose and objective were to unite all the best skills and experience of both the departments of Radiology and Cardiovascular Disease to set a new standard and paradigm of clinical excellence.

The marriage of the power of ^{13}N-Ammonia with the groundbreaking and breathtaking resolution, sensitivity, speed, and efficiency of the all-digital Discovery MI was nearly unprecedented for this application.

Next, we established the "on-demand" credibility, capability, reliability and reach of the product yield of ^{13}N-Ammonia through carefully choreographed dry runs. Once this was assured, the MPI stress protocol was built around the goal of maximum operational efficiency of patient flow and throughput.

We chose Regadenoson for pharmacological stress for its safety profile, ease of utilization, standard dosing regardless of BMI, and its reliability through a single IV line utilized for both tracer and stress agent.

We built into the protocol a 60-90 second delay between the completion of Regadenoson infusion and the administration of the stress dose of tracer so as to acquire time-activity curves for flow quantification during the peak of coronary flow reserve.

A low-dose rest/high-dose pharmacologic stress protocol was developed and designed to maximize patient comfort and minimize the duration of the exam. Initially, we tested both separate rest and stress acquisition, but ultimately found the performance both of rest and stress in a single session were well tolerated by the vast majority of patients. It also simplified the test by eliminating downloading and uploading of the patients onto the imaging table and shorted the overall process in all patients. Both rest and stress imaging were performed without removing the patient from the PET/CT table. Just prior to rest and post-stress, a low-dose free-breathing CT scan was obtained for attenuation correction. Total duration of the exam from rest dose injection to conclusion of the post-stress CT attenuation scan was uniformly 30 minutes or less.

By design, a predetermined dose of ^{13}N-Ammonia was injected as a resting dose on the top of the hour and the Regadenoson stress dose exactly to follow at 15-20 minutes past the hour. Doses were calibrated to deliver a 4:1 dosing differential at the time of stress compared to the residual activity still present at rest after completion of the resting image acquisition. For example, a 5mCi resting dose with a subsequent 10-minute image acquisition results in only 2.5mCi of residual activity before a 10mCi stress dose injection and image acquisition. Even further radiation dose reduction and optimization is possible, with the newer all-digital scanners promising extremely low effective doses to the patient compared to ^{82}Rb or standard SPECT tracers. Our protocol was established by an iterative process searching for the lowest resting dose that could be delivered without compromising image quality and quantification of myocardial resting flow while also administering a stress dose high enough not to be compromised by residual baseline activity. Incredibly, using the all-digital Discovery MI scanner, resting injected doses of as low as 2 mCi yielded adequate images for interpretation and flow quantification.

For ease of the testing and technologist work flow, the tracer injections were designed to be delivered by handheld injection over 20 seconds followed by a 20 ml saline bolus to flush the venous system.

This resulted in a typically reproducible first pass time-activity curve in most patients with a peak count rate of about 1,200 kcounts/second (kcps).

Similarly, the stress high dose typically reached a peak count rate on the time-activity curve of approximately 9-14,000 kcps or more. Just prior to stress tracer injection, the typical baseline activity ranged about 100-200 kcps. If not, the stress dose was slightly delayed achieving this goal. Detector saturation was not encountered in any patient. During phantom studies, up to 19,000 kcps were achieved without detector saturation. The true upper dose limit of the Discovery MI platform before detector saturation has yet to be defined with ^{13}N-Ammonia.

The time interval between doses was set by a prescribed ^{13}N-Ammonia product delivery schedule. Each dose was the product of its own beam run time and synthesis process. Doses achieved for patients were not constrained by the synthesis efficiency.

Scan acquisitions times were set to 10 minutes for rest and 10 minutes for stress. List mode acquisition was employed in all cases with EKG gating. static and dynamic rebinning for all patients.

A key design component of the strategy was to set trace dose delivery times and manage patient flow to match the dose schedule. We found this to compact and minimize the table time for the patient to the bare minimum, likely improving tolerance of the patients to the procedure.

The cases selected were constrained by the requirement that patients abstain from medicines and products containing caffeine for at least 12 hours.

During this interval, serial enzymes were obtained, and patient monitored on telemetry.

Patients with documented STEMI were not included.

During this interval, only a single ^{13}N-Ammonia dose was missed from its delivery on schedule. In this case, a resting scan was deferred, and the stress-only dose was performed on schedule according to protocol. In the case of a normal stress scan, follow-up resting images are not required, allowing the patient a prompt clinical decision and, if appropriate, early discharge.

Myocardial blood flow at rest and at peak stress as well as myocardial flow reserve were quantitated on all patients and included in the interpretive report along with the stress EKG findings.

In all cases, the studies were completed and interpreted before noon.

Compared to standard SPECT operating condition, the length of stay for this indication was shortened by approximately 4-6 hours.

Volume performance was only limited by room clean-up and patient off-loading. Transportation demands are high, requiring patient delivery to the scanner precisely on schedule in order to meet the prearranged ^{13}N-Ammonia synthesis production strategy.

Nursing requirements were not different from standard SPECT MPI operating procedures.

Interpretation was performed with QPS+QGS artificial intelligence software program from Cedars-Sinai with motion correction and utilizing gender matched ^{13}N-Ammonia normal control datasets. The rate-pressure product was used to adjust resting myocardial blood flow measurements.

Outcomes:

Under these conditions and constraints, we reviewed the first 50 consecutive patient cases:

Demographics:

Gender: 64% female.
Age: 66 +/- 11 years, range 43-89
BMI: 30.2 +/- 8.0, range 18.7-53

Statistical analysis:

Using a heuristic analysis, there were no false negatives studies. Of the first 50 cases, there were 8 subsequent invasive catheterizations: 4 required percutaneous coronary intervention (PCI), 3 others had coronary artery disease (CAD) but was treated by medical management only. A single case showed no CAD and was deemed a false positive by image analysis but was a true negative according to myocardial blood flow quantitative data. The decision to cath this patient was made by the referring physician's preference, pointing out the opportunity for further enhancement that may be achieved by educating referring physicians regarding the power of myocardial blood flow quantification as it impacts optimization of clinical decision-making for each patient.

Surprisingly, in retrospect analysis, 9.8% of the patients had detectable caffeine levels in blood samples drawn immediately prior to the study even with the strict adherence and compliance measures instituted in this exclusively inpatient population. This may simply reflect the prevalence of slow caffeine metabolizers or surreptitious patient noncompliance. In each of these cases, myocardial blood flow and myocardial flow reserve metrics were normal, indicating that at least at these low levels of caffeine, coronary blood flow reserve is not significantly impeded. None of these patients required cath and were discharged without further coronary testing.

Bottlenecks and Barriers:

Under this regimen, we found the patient transport systems and scanner availability to be the only patient volume limiting steps, but the exams were not constrained by limitation in the production and delivery of the product ^{13}N-Ammonia. Further schedule coordination is actively being pursued with the scheduled oncology patient volume. Expanded hours of operation are also being considered to improve access, utilization, and growth.

An unanticipated problem was the relatively frequent case, about 5 out of 100, in which patients refused to be imaged due to claustrophobia or inability or unwillingness to lay recumbent and still for 30 minutes. In some cases, exams were performed without complication by administering Ativan 1 mg iv. on call to the PET/CT lab. This highlights the importance of screening patients ahead of time for significant claustrophobia. Ativan was not administered to any patient in the PET/CT lab itself.

As noted above, there were a surprising number of patients with detectable caffeine in their blood samples drawn immediately prior to the imaging study as part of a quality assurance initiative. Notably, all these patients had normal resting and peak stress myocardial blood flow and myocardial flow reserve, indicating there exists a determinant blood level of caffeine that is acceptable and that does not significantly impede myocardial blood flow or flow reserve. The cost of testing blood caffeine levels was $29 per sample to the hospital but required the samples to be sent to an outside lab. Results were not known until the following day. Point-of-care caffeine level testing might have significant utility if it were available.

A physician and registered nurse trained in Advanced Cardiac Life Support and experienced with Regadenoson stress SPECT MPI were present at each exam. Aminophylline was administered to reverse the symptoms of Regadenoson in about 20% or less of the patients but was withheld until the completion of at least the first 5 minutes of scan time after stress dose tracer injection.

Orders for the studies were entered into the electronic medical record by 7:00 AM the morning of the exams. In the case where patients were unable to accommodate the scanner, inpatient substitutes were immediately generated on the fly from the pool of inpatients already assigned to standard SPECT MPI given that the preparation and protocols were identical between these modalities. The interpreting physician's report of the exam were generated immediately as the studies were processed and targeted to be in the electronic medical record by the noon hour. Studies were limited to the morning hours and not performed after 11:30 AM.

There was one case of Mobitz Type 2 AV block that occurred with Regadenoson stress which was transient and did not require reversal and spontaneously resolved. There were two other case of severe bradycardia that respond to aminophylline but did not require discontinuation of the exam.

Finally, in the process of program development and implementation, it was apparent to us, as others have observed, that a ^{13}N-Ammonia PET/CT MPI program requires an identifiable single physician "champion" willing to direct and sustain its development.

Conclusion

In summary, physicians faced with a patient complaining of chest pain in the ED, or in the clinic, are presented with an existentially and economically pressing turning point in the clinical pathway. A misinformed decision at this point will carry life-threatening unintended consequences. The physician needs timely access to the critically important data provided by noninvasive imaging of coronary artery perfusion. The ideal methodology employed must be of the highest non-invasive diagnostic accuracy and the lowest reasonably achievable radiation exposure to the patient. Based upon fundamental principles, ^{13}N-Ammonia pharmacological stress MPI-PET/CT has the "**best in class**" tracer characteristics needed to meet this standard. It is better than ^{82}RbCl, better than ^{99m}Tc isonitriles, better than ^{201}TlCl SPECT MPI, has better radiation dosimetry than CCTA, ^{18}F-flurpiridaz or invasive coronary catheterization, and has wider utility than pharmacological stress echocardiography. Availability of the new all-digital PET/CT scanner technology offers an ideal opportunity for optimizing utilization of this modality and promises further reduction in the effective doses of radiation delivered to the patient and technical staff.

References:

1. Rosamond T. Initial appraisal of acute coronary syndrome. Understanding the mechanisms, identifying patient risk. *Postgraduate Medicine*, July 2002:112:29-42.
2. Weigold WG, Coronary Computed Tomography in the Emergency Department. The High Stakes Game of Low Risk Chest Pain. *JACC* Vol.61, No.8, 2013.
3. Christenson J, et al. Safety and efficiency of emergence department assessment of chest discomfort. i 2004; 170:1803-7.
4. Pope JH, et al. Missed diagnosis of acute cardiac ischemia in the emergency department. i 2000; 342:1163-70.
5. Strauss WH, Baily D. Resurrection of Thallium-201 for Myocardial Perfusion Imaging. i. 2009; 2(3) 283-285.
6. Leppo JA and Meerdink DJ. Comparison of the Myocardial Uptake of a Technetium-Labeled Isonitrile Analogue and Thallium. *Cir. Res*. 1989; 65:632-639.
7. Einstein AJ, Moser KW, Thompson RC, Cerquerira MD, Henzlova MJ. Radiation dose to the patient from cardiac diagnostic imaging. *Circulation* 2007; 116:1290-1305.
8. Leppo JA. Comparison of pharmacological stress agents. *J Nucl Cardiol*. 1996;3: S22-S26.
9. Salerno M, Beller GA. *Cir Cardiovasc Imaging*. 2009; 2:412-424.
10. Maddahi J. SPECT and PET MPI. Physiological basis and acquisition protocols. ASNC 2010 presentation.

11. Taillefer R and Wackers FJT. "Kinetics of conventional and new cardiac radiotracers from *Nuclear Cardiac Imaging. Principles and Applications*. 5th edition. Ed. Iskandrian and Garcia Oxford University Press 2016, 198 Madison Avenue, New York, NY 10016
12. Salerno M. Noninvasive assessment of myocardial perfusion. *Circ Cardiovasc Imaging*. 2009 Sep;2(5):412-24.
13. Courtney M. Triple rule out: why it is not ready to roll out. *Acad Emerg Med*. 2013 Sep;20(9):934-6.
14. Landry A. Should triple rule-out CT angiography be used in patients with suspected acute coronary artery disease, aortic dissection, or pulmonary embolus? *Ann Emerg Med*. 2015 Feb;65(2):216-7.
15. Rosamond T. Protocol: *Coronary CT-Triple Rule-Out Angiography: Patient Algorithm for Chest Pain in the CTU.* March 30, 2015.
16. Gruettner J. Clinical assessment of chest pain and guidelines for imaging. *Eur J Radiol.* 2012 Dec;81(12):3663-8.
17. Gruettner J. Coronary computed tomography and triple rule out CT in patients with acute chest pain and an intermediate cardiac risk profile. Part 1: impact on patient management. *Eur J Radiol.* 2013 Jan;82(1):100-5.
18. Takakuwa KM. A meta-analysis of 64-section coronary CT angiography findings for predicting 30-day major adverse cardiac events in patients presenting with symptoms suggestive of acute coronary syndrome. *Acad Radiol*. 2011 Dec;18(12):1522-8.
19. Weigold G. Coronary Computed Tomography Angiography in the Emergency Department. *JACC*. Feb 2013, 61 (8) 893-895.
20. Staniak H. Coronary CT angiography for acute chest pain in the emergency department. *J Cardiovasc Comput Tomogr.* 2014 Sep-Oct;8(5):359-67.
21. Gaemperli O. Interaction of Caffeine with Regadenoson-Induced Hyperemic Myocardial Blood Flow as Measured by Positron Emission Tomography. *JACC*. Jan 2008, 51 (3) 328-329.
22. Samad Z. A meta-analysis and systematic review of computed tomography angiography as a diagnostic triage tool for patients with chest pain presenting to the emergency department. *J Nucl Cardiol*. 2012 Apr;19(2):364-76.
23. Goldstein J. The CT-STAT (Coronary Computed Tomographic Angiography for Systematic Triage of Acute Chest Pain Patients to Treatment) trial. *J Am Coll Cardiol*. 2011 Sep 27;58(14):1414-22.
24. Litt H. CT Angiography for Safe Discharge of Patients with Possible Acute Coronary Syndromes. *N Engl J Med*. 2012; 366:1393-1403.
25. Goldstein J. A randomized controlled trial of multi-slice coronary computed tomography for evaluation of acute chest pain. *J Am Coll Cardiol*. 2007 Feb 27;49(8):863-71.
26. Dorbala S, Slmoka P, et al. *Clinics Review Articles: Cardiology Clinics.* February 2016.
27. Wei Q. Intrinsic Radiation in Lutetium Based PET Detector: Advantages and Disadvantages. *arXiv*:1501.05372 [physics.ins-det].
28. Lightburst Digital Detector: A Whitepaper. https://www.gehealthcare.com/-/media/91ceb1d3e40248a9bb9d6e4b733ddff1.pdf.
29. Iskandrian A. Pharmacologic stress testing: mechanism of action, hemodynamic responses, and results in detection of coronary artery disease. *J Nucl Cardiol*. 1994 Jan-Feb;1(1):94-111.
30. Maddahi J. Properties of an ideal PET perfusion tracer: new PET tracer cases and data. *J Nucl Cardiol*. 2012 Feb;19 Suppl 1:S30-7.
31. *Cardiac PET and PET/CT Imaging Practice Guidelines A summary of the recommendations and practice guidelines of professional groups.* http://snmmi.files.cms-plus.com/docs/PET_PROS/CardiacPracticeGuidelinesSummary.pdf.

32. Cheng K. [^{13}N]Ammonia: [^{13}N]NH_3. 2005 Dec 5 [Updated 2007 Dec 4]. In: *Molecular Imaging and Contrast Agent Database* (MICAD) [Internet]. Bethesda (MD): National Center for Biotechnology Information (US); 2004-2013.
33. Adeva M. Ammonium metabolism in humans. *Metabolism*. 2012 Nov;61(11):1495-511.
34. Alessio A. Validation of an axially distributed model for quantification of myocardial blood flow using ^{13}N-ammonia PET. *J Nucl Cardiol*. 2013 Feb;20(1):64-75.
35. Beller G. Quantification of myocardial blood flow with PET: ready for clinical application. *J Nucl Cardiol*. 2012 Oct;19(5):877-8.
36. Saraste A. PET: Is myocardial flow quantification a clinical reality? *J Nucl Cardiol*. 2012 Oct;19(5):1044-59.
37. Murthy V. Noinvasive quantification of coronary vascular dysfunction for diagnosis and management of coronary artery disease. *J Nucl Cardiol*. 2012 Oct;19(5):1060-72.
38. Dilsizian V. ASNC imaging guidelines/SNMMI procedure standard for positron emission tomography (PET) nuclear cardiology procedures. *J Nucl Cardiol*. 2016 Oct;23(5):1187-1226.
39. Dilsizian V. Pet myocardial perfusion and metabolism clinical imaging. *JACC*. 2009 August; 16(4): 651.
40. Bacharach S. PET myocardial glucose metabolism and perfusion imaging: Part 1-Guidelines for data acquisition and patient preparation. *J Nucl Cardiol*. 2003 Sep-Oct;10(5):543-56.
41. Herzog B. Long-term prognostic value of 13N-ammonia myocardial perfusion positron emission tomography added value of coronary flow reserve. *J Am Coll Cardiol*. 2009 Jul 7;54(2):150-6.
42. Mattsson S. Radiation Dose to Patients from Radiopharmaceuticals. *Annals of the ICRP*, 44(2_suppl), 7–321.
43. Cremer P. Risk stratification with exercise N (13)-ammonia PET in adults with anomalous right coronary arteries. *Open Heart*. 2016 Aug 22;3(2): e000490.
44. Nakazato R. Myocardial perfusion imaging with PET. *Imaging Med*. 2013 Feb 1; 5(1): 35–46.
45. Cremer P. Risk stratification with exercise N (13)-ammonia PET in adults with anomalous right coronary arteries. *Open Heart*. 2016 Aug 22;3(2): e000490.
46. Tamaki N. et al. Value and limitation of Thallium-201 single photon emission computed tomography: Comparison with Nitrogen-13 ammonia Positron Tomography. *J Nucl Med* 29:1181-1188, 1988.
47. Schelbert HR, et al. Regional myocardial perfusion assessed with N-13 labeled ammonia and positron emission computerized axial tomography. *Am J Cardiol* 1979; 43:209-218
48. Schelbert HR, et al. N-13 ammonia as an indicator of myocardial blood flow: factors influencing its uptake and retention in myocardium. *Circulation* 1981; 63:1259-1272.
49. Schelbert HR, et al. Noninvasive assessment of coronary stenosis by myocardial imaging during pharmacologic coronary vasodilatation. VI. Detection of coronary artery disease in human beings with intravenous N-13 ammonia and positron computed tomography. *Am J Cardiol* 1982; 49:1197-1207.
50. Wisenberg G, et al. In vivo quantification of regional myocardial blood flow by positron-emission computed tomography. *Circulation* 1981; 63:1248-1258.
51. Tamaki N, et al. Myocardial positron computed tomography with 13N-ammonia at rest and during exercise. *Eur J Nucl Med* 1985; 11:246-251.
52. Yonekura Y, et al. Detection of coronary artery disease with 13 N-ammonia and high-resolution positron-emission tomography. *Am Heart J* 1987; 113:645-654.
53. Senda M, et al. Interpolating scan and oblique-angle tomograms in myocardial PET using N-13 ammonia. *J nucl Med* 1986; 27: 1836-1980.

54. Bergmann SR, et al. The dependence of accumulation of 13NH3 by myocardium on metabolic factor and its implication for quantitative assessment of perfusion. *Circulation* 1981; 61:34.
55. Laubenbacher C, et al. An automated analysis program for the evaluation of cardiac PET studies: Initial results in the detection and localization of coronary artery disease using nitrogen-13-ammonia. *J Nucl Med* 1993; 34: 968-978.
56. Muzik O, et al. Assessment of diagnostic performance of quantitative flow measurements in normal subjects and patients with angiographically documented coronary artery disease by means of Nitrogen-13 ammonia and positron emission tomography. *J Am Coll Cardiol* 1998; 534-540.
57. Nandar M, et al. Integrated PET/CT foe the assessment of coronary artery disease. A feasibility study. *J Nucl Med* 2005; 46:930-935.
58. Glover D, et al. Journey to find the ideal PET flow tracer for clinical use: Are we there yet? *J Nucl Cardiol* 2007; 14:765-8.
59. Leppo J. Comparison of pharmacologic stress agent. *J Nucl Cardiol* 1996;3: S22-S26.
60. Nandalur K, et al. Diagnostic performance of Positron Emission Tomography in the detection of coronary artery disease: A Meta-analysis. *Acad Radiol* 2008; 15:444-451.
61. Dilsizian V, et al. ASNC imaging guidelines/SNMMI procedure standard for positron emission tomography (PET) nuclear cardiology procedures. *J Nucl Cardiol* 2016.
62. Hickey KT, et al. An improved model for the measurement of myocardial perfusion in human beings using N-13 ammonia. *J Nucl Cardiol*. 2005;12(3):311-7.
63. Khorsand A, et al. Gated Vardiac 13 N-NH3 PET for Assessment of Left Ventricular Volumes, Mass, and Ejection Fraction: Comparison with Electrocardiography-Gated 18F-FDG PET. *J Nucl Med*. 2005;46(12):2009-13.
64. Schepis T, et al. Absolute quantification of myocardial blood flow with 13 N-ammonia and 3-dimensional *PET*. *J Nucl Med*. 2007;48(11)1783-9.
65. Alessio AM, et al. Validation of an axially distributed model for quantification of myocardial blood flow using 13n-ammonia PET. *J Nucl Cardiol* 2013; 20:64-75.
66. Herzog B, et al. Long term prognostic value of 13N-ammonia myocardial perfusion positron emission tomography. *J Am Coll Cardiol* 2009; 54:150-6.
67. Fiechter M, et al. Diagnostic value of 13 N-ammonia myocardial perfusion PET: Added value of myocardial flow reserve. *J Nucl Med 2012*; 53:1230-1234.
68. Kajander SA, et al. Clinical value of absolute quantification of myocardial perfusion with ^{15}O-water in coronary artery disease. *Cir Cardiovasc Imaging* 2011;4(6):678-84.
69. Fiechter M, et al. Diagnostic value of 13 N ammonia myocardial perfusion PET: added value of myocardial flow reserve. *J Nucl Med*. 2012;53(8):1230-4.
70. Hajjiri MM et al. Comparison of positron emission tomography measurement of adenosine-stimulated absolute myocardial blood flow versus relative myocardial tracer content for physiological assessment of coronary artery stenosis severity and location *J Am Coll Cardiol*. 2009;54(2):751-8.
71. Herzog BA, et al. Long term prognostic value of 13 N-ammonia myocardial perfusion positron emission tomography added value of coronary flow reserve. *J Am Coll Img*. 2009;2(6):150-6.
72. Arsanjani R, et al. Comparison of fully automated computer analysis and visual scoring for detection of coronary artery disease from myocardial perfusion SPECT in a large population. *J Nucl Med*. 2013 Feb; 54(2):221-228.
73. Tio RA, et al. Comparison between the prognostic value of left ventricular function and myocardial perfusion reserve in patients with ischemic heart disease. *J Nucl Med*. 2009;50(2):214-9.
74. Xu Y, et al. Automatic and visual reproducibility of perfusion and function measures for myocardial perfusion SPECT. *J Nucl Cardiol*. 2010 Dec;17(6):1050-1057.

75. Dupuy EG, et al. 2012, ASNC Preferred Practice Statement-Patient Centered Imaging. *J Nucl Cardiol*. https://www.asnc.org/files/PCI%202012.pdf
76. Dilsizian V, et al. Quantitative PET myocardial blood flow. "Trust But Verify" JACC: *Cardiovascular Imaging*. Vol.10, No. 5. 2017.
77. Slomka PJ, et al. Comparison of clinical tools for measurement of regional stress and rest myocardial blood flow assessed with 13N-ammonia PET/CT. *J Nucl Med*. 2012 Feb;53(2):171-181.
78. Klingensmith WC, et al. Decreased perfusion in the lateral wall of the left ventricle in PET/CT studies with 13N-ammonia: evaluation in healthy adults. *J Nucl Med Technol*. 2009 Dec;37(4):215-219.
79. Patel MR, et al. Low Diagnostic Yield of Elective Coronary Angiography. *N Engl J Med* 2010; 362:886-895
80. Vavalle J, et al, Effect of the Presence and Type of Angina on Cardiovascular Events in Patients Without Known Coronary Artery Disease Referred for Elective Coronary Angiography *JAMA* Cardiol. 2016; 1(2): 232-234.
81. El Fakhri G, et al. Reproducibility and accuracy of quantitative myocardial blood flow assessment with (82)Rb PET: Comparison with (13)N-ammonia PET. *J Nucl Med*. 2009 Jul;50(7):1062-71.
82. Murthy V, et al. Clinical quantification of myocardial blood flow using PET: Joint position paper of the SNMMI cardiovascular council and the ASNC. *J Nucl Med*. 2018 Feb;59(2):1-21.
83. Dorbala S, Blankstein R, Skali H, Park M-A, Fantony J, Mauceri C, et al. Approaches to reducing radiation dose from radionuclide myocardial perfusion imaging. *J Nucl Med* (2015) 56:592–9.
84. Senthamizhchelvan S, Bravo PE, Esaias C, Lodge MA, Merrill J, Hobbs RF, et al. Human biodistribution and radiation dosimetry of 82Rb. *J Nucl Med* (2010) 51:1592–9.10.